

Hadronic and Quark-Gluon Excitations of Dense and Hot Matter*

T. Renk^a, R.A. Schneider^a and W. Weise^{a,b}

^aPhysik Department, Technische Universität München, D-85747 Garching, Germany

^bECT*, Villa Tambosi, I-38050 Villazzano (Trento), Italy

We summarize recent developments in our understanding of low-mass quark-antiquark excitations in hadronic matter under various different conditions. This includes the thermodynamics of the chiral condensate, pions as Goldstone bosons in normal nuclear matter, and excursions into extreme territory of the QCD phase diagram: lepton pair production from a fireball expanding through the transition boundary between the quark-gluon and hadron phases of QCD.

1. Phases of QCD

Exploring the QCD phase diagram is undoubtedly one of the great challenges in the physics of strong interactions. At temperatures exceeding $T_C \simeq \Lambda_{QCD} \sim 0.2$ GeV, one expects a plasma of quarks and gluons released from their confining forces. At $T < T_C$ and at moderate baryon densities, the relevant QCD degrees of freedom are color-singlet hadrons. Chiral symmetry is spontaneously broken. The vacuum is a condensate of scalar quark-antiquark pairs. Pions act as Goldstone bosons. Their decay constant, $f_\pi = 92.4$ MeV, determines the chiral scale $4\pi f_\pi \sim 1$ GeV which governs the low mass hadron spectrum. The lightest vector mesons (ρ, ω) can be seen as the lowest $q\bar{q}$ "dipole" excitations of the QCD vacuum. Current algebra combined with QCD sum rules [1] connects their masses directly with the chiral scale, $\sqrt{2}m_V = 4\pi f_\pi$, to leading order (and in the large N_c limit).

Evidently, investigating the changes of the spectral distributions of pseudoscalar and vector (as well as axial vector) excitations of the QCD vacuum with changing temperatures and baryon densities, from moderate to extreme, is a key to understanding QCD thermodynamics, its phases and symmetry breaking patterns.

2. Chiral thermodynamics: selected topics

A central point in the discussion of the QCD phase diagram is the transition from the Nambu-Goldstone realization of chiral symmetry (with non-zero condensate $\langle \bar{q}q \rangle$) to the "restored" Wigner-Weyl realization in which the chiral condensate vanishes. Lattice QCD indicates that chiral restoration is probably linked to the transition between composite hadrons and deconfined quarks and gluons.

*Invited talk presented by W. Weise at the 3rd International Conference on Perspectives in Hadron Physics, ICTP, Trieste, 7-11 May 2001; Work supported in part by BMBF, GSI and DFG.

Spontaneous chiral symmetry breaking (together with explicit breaking by the small u - and d -quark masses, $m_{u,d} < 10$ MeV) implies the PCAC or Gell-Mann, Oakes, Renner (GOR) relation, $m_\pi^2 f_\pi^2 = -m_q \langle \bar{q}q \rangle$, to leading order in the quark mass $m_q = (m_u + m_d)/2$. The GOR relation continues to hold [2] in matter at finite temperature $T < T_C$ and baryon density ρ , when reduced to a statement about the *time* component of the axial current. For this component we denote the corresponding in-medium pion decay constant by $f_\pi^*(\rho, T)$. One finds [2]

$$f_\pi^{*2}(\rho, T) m_\pi^{*2} = -m_q \langle \bar{q}q \rangle_{\rho, T} + \dots, \quad (1)$$

where $\langle \bar{q}q \rangle_{\rho, T}$ now stands for the T - and ρ -dependent chiral condensate. The "melting" of this condensate by heat or compression therefore translates primarily into an in-medium change of the (timelike) decay constant of the pion, given that its in-medium mass m_π^* is not much different from m_π in vacuum, because of its Goldstone boson nature.

The chiral scale, $4\pi f_\pi^*(\rho, T)$, is expected to decrease when thermodynamic conditions change toward chiral restoration. This scale defines a gap in the low-energy hadron spectrum. A decreasing chiral gap should imply characteristic observable changes in the meson mass spectrum.

Fig. 1 shows typical examples of calculated vector meson spectral distributions in nuclear matter at $T = 0$ and, in contrast, their evolution with temperature at zero baryon density. Such spectra are used in calculations of lepton pair production rates from ultrarelativistic heavy-ion collisions as described in later sections. The main part of this presentation focuses on the quest for signals of the QCD equation of state through dilepton radiation from hot matter. Before exploring such extreme territory, we summarize two topics of current interest in chiral thermodynamics at more moderate conditions.

2.1. Thermodynamics of the chiral condensate

Suppose we start from a chiral effective Lagrangian, appropriate for the hadronic phase of QCD, with Goldstone bosons (pions) coupled to baryons (nucleons). Let \mathcal{Z} be the partition function derived from this theory, and μ the baryon chemical potential. The pressure is $p(\mu, T) = (T/V) \ln \mathcal{Z}$, where V is the volume. Given this equation of state, a variant of the Hellmann-Feynman theorem (with the quark mass treated formally as an adiabatic parameter) in combination with the GOR relation leads to the following density and temperature dependent chiral condensate [3]:

$$\frac{\langle \bar{q}q \rangle_{\rho, T}}{\langle \bar{q}q \rangle_0} = 1 + \frac{dp(\mu, T)}{f_\pi^2 dm_\pi^2} = 1 + \frac{1}{f_\pi^2} \left[\frac{\partial p(\mu, T)}{\partial m_\pi^2} - \frac{\sigma_N}{m_\pi^2} \rho_S(\mu, T) \right], \quad (2)$$

with the baryon and scalar densities, $\rho = \partial p / \partial \mu$ and $\rho_S = -\partial p / \partial M$, and the nucleon sigma term $\sigma_N = m_q \partial M / \partial m_q \simeq 0.05$ GeV, where M is the nucleon mass.

At $T = 0$ we have $m_q [\langle \bar{q}q \rangle_\rho - \langle \bar{q}q \rangle_0] = \sigma_N \rho_S$. At low baryon density where $\rho_S \simeq \rho$, the magnitude of the condensate decreases linearly with density. This behaviour persists up to about the density of normal nuclear matter. Detailed calculations using self-consistent thermal effective field theory at the two-loop level [3,4] show that effects non-linear in ρ take over at higher density such that the rapid decrease of $|\langle \bar{q}q \rangle_\rho|$ is slowed down.

The temperature dependence of the condensate at $\rho = 0$ is determined by thermal pion fluctuations. The result of our recent calculations [3,4] is close to that found in chiral

perturbation theory [5] and quite similar to the result of lattice QCD [6], with a critical temperature $T_C \simeq 180$ MeV (for two flavours). The tendency towards "chiral restoration" indicated by the dropping condensate should have observable consequences, not only at extreme densities and temperatures, but also already in normal nuclear systems.

2.2. Pionic s -waves in the nuclear medium

Let us have a brief look at Goldstone bosons in the medium. In the exact chiral limit with $m_q = 0$, pions are massless, and this feature persists at all temperatures and densities as long as one stays within the Nambu-Goldstone phase of spontaneously broken chiral symmetry. Explicit symmetry breaking causes characteristic deviations from this pattern. They become particularly interesting in highly asymmetric nuclear matter, with large excess of neutrons over protons.

There has been a recent revival of interest in s -wave pion-nucleus interactions, for several reasons. First, the observation of deeply bound pionic atom states in Pb isotopes [7] has sharpened the quantitative constraints on the s -wave optical potential. Secondly, there is renewed interest in the theoretical foundations of this optical potential from the point of view of chiral dynamics [3,8,9].

To leading chiral order, at $T = 0$ and in the low density limit, the self-energy for a π^+ or π^- at low energy ω and momentum $\vec{q} = 0$ is simply given by the Weinberg-Tomozawa theorem:

$$\Pi^\pm(\omega, \vec{q} = 0) = \pm \frac{\omega}{2f_\pi^2}(\rho_p - \rho_n) + \dots, \quad (3)$$

so that the primary medium effect is a splitting of the π^+ and π^- masses, $\Delta m(\pi^\pm) = \pm(\rho_p - \rho_n)/4f_\pi^2$, in asymmetric nuclear matter. Systematic calculations of the π^+ and π^- mass shifts up to two-loop order using in-medium chiral perturbation theory [9] predict $\Delta m(\pi^-) \simeq 14$ MeV and $\Delta m(\pi^+) \simeq -1$ MeV at nuclear matter density and at a neutron-to-proton ratio $N/Z = 1.5$ characteristic of the Pb region. The repulsive shift found for the π^- mass is however only half of what is required by the data on deeply bound ($1s$ and $2p$) states in pionic Pb [7]. Several options to repair this discrepancy exist. We believe [3] that an appealing one is the reduction of the pion decay constant in medium, following eq. (1). The replacement $f_\pi \rightarrow f_\pi^*$ in the pion self-energy comes naturally because in-medium chiral perturbation theory must now be performed relative to a modified vacuum with shifted chiral condensate. Systematic investigations of deeply bound pionic atoms with various isotopic chains of heavy nuclei will provide further insights into these challenging questions.

3. Dilepton production rates and thermal QCD

Lattice simulations with three light quark flavours indicate that QCD undergoes a phase transition at a temperature $T_C \sim 150$ MeV [10]. It is hoped that it is possible to create the quark-gluon plasma (QGP) phase above T_C in ultrarelativistic heavy-ion collisions at CERN and RHIC. Dileptons (e^+e^- and $\mu^+\mu^-$ pairs) are interesting probes in this context since they do not interact strongly but escape unthermalized from the hot and dense region formed in such collisions, the fireball. As the fireball expands, it cools off and hadronization sets in at T_C . In the hadronic phase, the main dilepton sources

are pion and kaon annihilation processes which are enhanced due to the formation of the light vector mesons ρ, ω and ϕ .

The differential dilepton emission rate from a hot domain in thermal equilibrium is given by

$$\frac{dN}{d^4x d^4q} = \frac{\alpha^2}{\pi^3 q^2} \frac{\text{Im}\bar{\Pi}(q, T)}{e^{q^0/T} - 1} \quad (4)$$

where $\bar{\Pi}$ denotes the spin-averaged time-like self energy of a photon in the heat bath, q is the photon four-momentum, $\alpha = \frac{e^2}{4\pi}$, and the lepton masses have been neglected. Later we compare our results with the CERES/NA45 data taken in Pb-Au collisions at 160 AGeV (corresponding to a c.m. energy of ~ 20 AGeV). This is done by integrating eq.(4) over the space-time history of the collision and, taking into account the experimental detector acceptance, over the transverse momentum p_T and average over the rapidity η .

3.1. Quasiparticle description of the quark-gluon phase

Thermal QCD perturbation theory is presumably not applicable to evaluate $\text{Im}\bar{\Pi}$, even at high temperatures. A way to proceed is to use input from finite temperature lattice simulations. We have shown recently [11] that it is possible to describe the equation of state (EoS) of such systems to a very good approximation in terms of a non-interacting gas of quasiparticles with thermally generated masses, incorporating confinement phenomenologically by a temperature-dependent effective number of active degrees of freedom.

From asymptotic freedom, we expect that at extremely high temperatures the plasma consists of quasifree quarks and gluons. Perturbative calculations find spectral functions of the form $\delta(\omega^2 - k^2 - m^2(T))$ with $m(T) \sim g_s T$. As long as the spectral functions of the thermal excitations at lower temperatures still resemble qualitatively this asymptotic form, a quasiparticle description is expected to be applicable. The thermal excitations can then be described by a dispersion relation $\omega^2(k) = k^2 + m^2(T)$.

We assume that the thermal quark and gluon quasiparticle masses still behave as $\tilde{g}(T)T$, with an effective coupling strength parametrized as

$$\tilde{g}(T) \simeq g_0 \left(1 - \frac{T_C}{T}\right)^\gamma. \quad (5)$$

This form is guided by lattice results which indicate that the phase transition is weakly first order or second order, suggesting approximately $m \sim (T - T_C)^\gamma$ with some "pseudocritical" exponent γ .

The second important element in this model is a temperature-dependent confinement factor which reduces the number of thermally active degrees of freedom as T approaches T_C . In practice, the quasiparticle parameters are determined by reproducing lattice results for the entropy density. The pressure and the energy density then follow accordingly and are in excellent agreement with lattice data whenever a comparison can be made [11].

In the quark-gluon phase, the basic mechanism that produces e^+e^- pairs is $q\bar{q}$ annihilation. Assume now that these quarks and antiquarks are thermal quasiparticles, and that these quasiparticles couple to photons in the same way as bare quarks. We can then use the standard one-loop result for $\text{Im}\bar{\Pi}$, with bare quark masses replaced by the thermal masses, $m_q(T)$. The essential QCD dynamics is supposed to be incorporated in these quasiparticle masses as they are in accordance with the lattice QCD equation of state.

3.2. The hadronic phase

Below T_C , confinement sets in and the effective degrees of freedom change to colour singlet, bound $q\bar{q}$ or qqq states. The photon couples now to the lowest-lying 'dipole' excitations of the vacuum, the hadronic $J^P = 1^-$ states: the ρ , ω and ϕ mesons and multi-pion states carrying the same quantum numbers. The electromagnetic current-current correlation function can be connected to the currents generated by these mesons using an effective Lagrangian which approximates the $SU(3)$ flavour sector of QCD at low energies. We use the *improved Vector Meson Dominance* model combined with chiral dynamics of pions and kaons as described in [12]. Within this model, the following relation between the imaginary part of the irreducible photon self-energy $\text{Im}\bar{\Pi}$ and the vector meson self-energies $\Pi_V(q)$ in vacuum is derived:

$$\text{Im}\bar{\Pi}(q) = \sum_V \frac{\text{Im}\Pi_V(q)}{g_V^2} |F_V(q)|^2. \quad (6)$$

Here g_V is the γV coupling constant and F_V is the form factor for the coupling of the vector meson to the multipion and $K\bar{K}$ continuum.

Finite temperature modifications of the vector meson self-energies appearing in eq.(6) are calculated using thermal Feynman rules. The explicit calculations for the ρ - and ϕ -meson can be found in ref.[13]. At the one-loop level, the ρ and ϕ are only marginally affected by temperature even close to T_C because of the comparably large pion and kaon masses: $m_\pi \simeq T_C$, $m_K \simeq 3 T_C$. The thermal spectral function of the ω -meson has been discussed in detail in [14]. Here, the reaction $\omega\pi \rightarrow \pi\pi$ was found to cause a considerable broadening of the ω spectral function, leading to $\Gamma_\omega(T_C) \simeq 7 \Gamma_\omega(0)$. The resulting photon spectral function is displayed in figure 1 (left panel). There is still considerable stopping

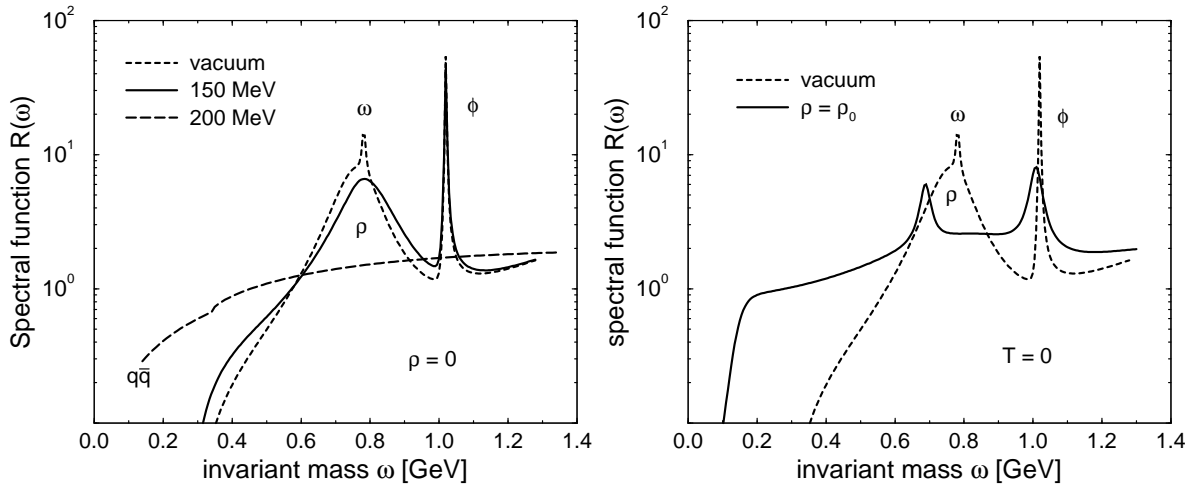


Figure 1. The photon spectral function $R(\omega) = -12\pi/\omega^2 \text{Im}\bar{\Pi}(\omega)$ at finite temperature and $\rho = 0$ (left panel), and at $T = 0$ and finite density (right panel). The $q\bar{q}$ line in the left panel shows the continuum spectral function in the quark-gluon phase for massless quarks.

of the interpenetrating nuclei at SPS energies, with a net baryon density ρ_B in the central rapidity region. At RHIC, on the other hand, first measurements indicate that finite baryon density effects should not play an important role. For the evaluation of density effects at SPS, we use the results discussed in [15]. The photon spectral function at finite density and zero temperature is depicted in figure 1 (right panel).

3.3. Fireball model

The fireball model is set up as follows: We assume a spatially averaged time and density profile throughout the evolution of the fireball at any given timeslice. Furthermore, we require the evolution of the system after the very initial stages to be isentropic. Given the value of the total entropy S_0 and the volume expansion of the fireball $V(t)$, the temperature profile $T(t)$ can then be constructed via the EoS of the system, depending on the relevant degrees of freedom. For temperatures above T_C , we use the results of the quasiparticle model described earlier. In the region below T_C , an interacting hadronic gas is an adequate description of the system. We parametrize our insufficient knowledge

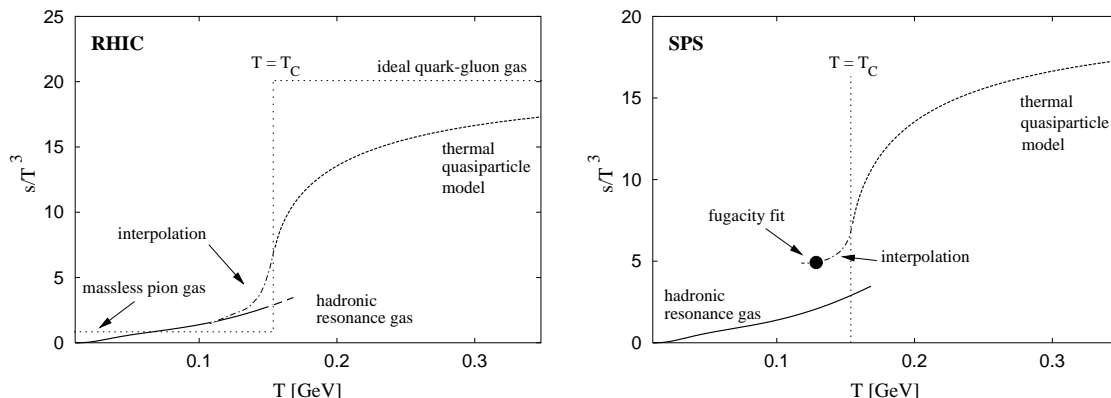


Figure 2. Left panel: The temperature dependence of the entropy density s in the RHIC scenario as compared to the ideal quark-gluon gas and the noninteracting massless pion gas limit (dotted). The three relevant regions used in the model calculation are given as ideal hadronic resonance gas (full), interpolation (dash-dot) and quasiparticle model (dashed). Right panel: Temperature dependence of the entropy density for SPS conditions, including the interpolation to the fugacity corrected value at freeze-out.

close to T_C by interpolating smoothly between two regimes. This approach is supported by the general shape of the EoS on the lattice for two light and one heavy quark, where a smooth crossover is indicated [16]. The entropy density in our model is shown in figure 2. Additionally, at SPS conditions, finite chemical potentials for mesons and baryons have to be taken into account. The evolution is stopped in the model as soon as a common freeze-out temperature $T_f \simeq 125$ MeV is reached. Given this basic framework, we adjust the remaining parameters of the model in such a way as to reproduce several hadronic observables such as the rapidity distribution of the produced hadrons, \mathbf{p}_t -spectra and particle ratios (for details see [17]).

3.4. Results

Initial temperatures are quite high in our approach (250 MeV for SPS conditions, 300 MeV for RHIC), and we find a significantly prolonged lifetime (10 fm/c at SPS and 15 fm/c at RHIC) of the QGP evolution phase of the fireball as compared to the results obtained by other groups [18]. This is a consequence of using the more realistic EoS of the thermal quasiparticle model rather than the one of the ideal quark-gluon gas.

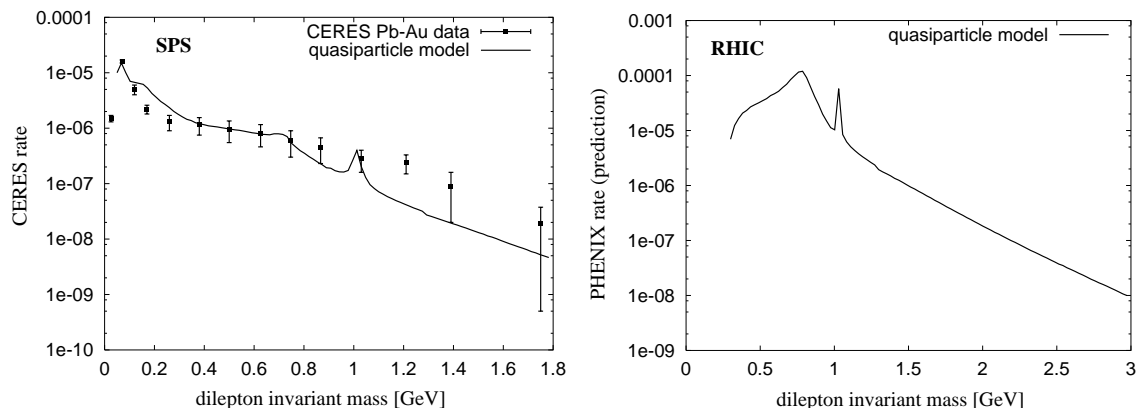


Figure 3. Dilepton invariant mass spectra for the SPS and RHIC conditions realized in the CERES/NA45 experiment [19] (data, upper panel) and the PHENIX detector (prediction, lower panel).

The results for the fully integrated dilepton rates are shown in figure 3. Comparing to the CERES experiment, the model achieves a good overall description. We are also able to describe the existing data in separate \mathbf{p}_t -regions (larger or smaller than 500 MeV).

In figure 4, the different stages of the fireball evolution building up the dilepton yield are resolved in small time steps. For early times, the only contribution comes from the $q\bar{q}$ quasiparticle annihilation processes out of the quark-gluon phase. The movement of the invariant mass threshold reflects the temperature dependence of the quasiparticle mass, which gets light near the phase transition at $t \sim 10$ fm. One observes that, in spite of the growing fireball volume, the contributions from later timeslices to the total QGP yield become successively less important. This behaviour is enforced by the confinement factor which reduces the thermodynamically active degrees of freedom near the phase boundary. For times later than 10 fm/c, the system enters the hadronic evolution phase without going through a mixed phase. The most prominent feature is the rapid filling of the low invariant mass region through the density-broadened ρ meson.

4. Summary

In our journey through different regions of the QCD phase diagram, we have first discussed the temperature and density dependence of the order parameter of spontaneous chiral symmetry breaking, the quark condensate. The in-medium evolution of this order parameter should manifest itself in a corresponding dropping of the pion decay constant.

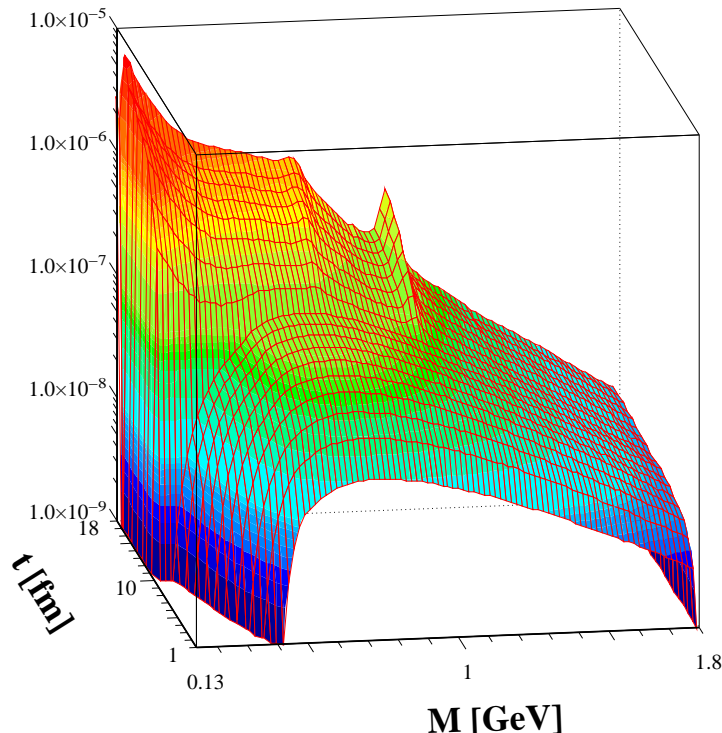


Figure 4. Time evolution of the (integrated) dilepton yield for the SPS scenario, as a function of dilepton invariant mass [17].

This in turn may lead to observable consequences for low-energy pion-nucleus interactions in systems with large neutron excess. New high-precision experiments producing deeply bound states of pionic atoms are a promising source of information to investigate these issues.

The major part of this presentation concentrated on the more extreme conditions encountered in heavy-ion collisions at CERN and RHIC. Signals of the expansion from a transient quark-gluon phase to the hadronic final states can in principle be observed by detecting lepton pairs from the expanding fireball produced in such collisions. We have emphasized the importance of using input and constraints from lattice QCD thermodynamics in the analysis of such signals.

We thank N. Kaiser, R. Rapp and J. Wambach for stimulating discussions.

REFERENCES

1. M. Golterman and S. Peris, Phys. Rev. **D 61** (2000) 034018; E. Marco and W. Weise, Phys. Lett. **B 482** (2000) 87.
2. V. Thorsson and A. Wirzba, Nucl. Phys. **A 589** (1995) 633; M. Kirchbach and A. Wirzba, Nucl. Phys. **A 604** (1996) 395; G. Chanfray, M. Ericson and J. Wambach, Phys. Lett. **B 388** (1996) 673.
3. W. Weise, in: Proceedings "Nuclei and Nucleons", Darmstadt, 2000, Nucl. Phys. **A** (2001), to appear, and refs. therein.
4. N. Kaiser, T. Schwarz and W. Weise, in preparation.
5. P. Gerber and H. Leutwyler, Nucl. Phys. **B 321** (1998) 387.

6. G. Boyd et al., Phys. Lett. **B 349** (1995) 170; F. Karsch, Nucl. Phys. (Proc. Suppl.) **B 83–84** (2000) 14.
7. H. Gilg et al., Phys. Rev. **C 62** (2000) 025201; K. Itahashi et al., Phys. Rev. **C62** (2000) 025202; T. Yamazaki et al., Z. Physik **A 335** (1996) 219.
8. T. Waas, R. Brockmann and W. Weise, Phys. Lett. **B 405** (1997) 215.
9. N. Kaiser and W. Weise, Phys. Lett. **B 512** (2001), 283.
10. F. Karsch, E. Laermann, A. Peikert, C. Schmidt and S. Stickan, Nucl. Phys. (Proc. Suppl.) **B 94** (2001) 411.
11. R.A. Schneider and W. Weise, hep-ph/0105242, subm. to Phys. Rev. C
12. F. Klingl, N. Kaiser and W. Weise, Z. Phys. **A356** (1996) 193.
13. R.A. Schneider and W. Weise, Eur. Phys. J. **A9** (2000) 357.
14. R.A. Schneider and W. Weise, Phys. Lett. **B** (2001), in print.
15. F. Klingl, N. Kaiser and W. Weise, Nucl. Phys. **A624** (1997) 527.
16. F. Karsch, plenary talk, Proceedings QM2001, to be published.
17. T. Renk, R.A. Schneider and W. Weise, preprint, submitted to Phys. Rev. **C**.
18. R. Rapp and J. Wambach, Eur. Phys. J. **A 6** (1999) 415; J. Sollfrank, P. Huovinen, M. Kataja, P. V. Ruuskanen, M. Prakash and R. Venugopalan, Phys. Rev. **C 55** (1997) 392; C. M. Hung and E. Shuryak, Phys. Rev. **C 57** (1998) 1891.
19. G. Agakichiev et al., Phys. Lett. **B 422** (1998) 405 and refs. therein.